Infrared and Raman studies of pressure-polymerized C_{60}

A. M. Rao and P. C. Eklund
Department of Physics and Astronomy and Center for Applied Energy Research, University of Kentucky, Lexington, Kentucky 40506

J-L. Hodeau and L. Marques
Laboratoire de Crystallographie, C.N.R.S., Boîte Postale 166 Cedex 09, 38042 Grenoble, France

M. Nunez-Regueiro
EPM-Matformag, C.N.R.S., Boîte Postale 166 Cedex 09, 38042 Grenoble, France

(Received 5 August 1996)

We discuss the room-temperature infrared and Raman spectra for the pressure-induced rhombohedral, tetragonal, orthorhombic C_{60} polymers and the C_{60} photopolymer. The interfullerene bonds are found to not only split the H_{1g}- and F_{1u}-derived modes, but also to soften these intramolecular modes relative to those in pristine solid C_{60}. The observed mode softening is attributed to the loss of C═C bonds in the molecular cages, which are broken to reform as intermolecular four-membered rings. Lorentzian line-shape analysis of the Raman data in the vicinity of the pentagonal pinch mode frequency in these polymerized structures reveals six distinct Raman lines at very nearly the same frequencies. However, the relative intensities of these lines were found to be sensitive to the phase of the fullerene polymers. The frequency of the $A_g(2)$- and the $F_{1u}(4)$-derived modes is found to depend linearly on the intermolecular coordinate a_I of the polymeric phases. A frequency softening of $\Delta\omega/\Delta a_I \sim 19$ and 58 cm^{-1}/Å was deduced for the $A_g(2)$- and the $F_{1u}(4)$-derived modes, respectively. In addition, the experimental spectra are compared to the vibrational spectra obtained from a first-principles molecular dynamical calculation for a C_{60} dimer and an infinite chain of polymerized C_{60}. [S0163-1829(97)08007-7]

I. INTRODUCTION

Since the first report on photoinduced polymerization in thin solid C_{60} films[1] there has been a surge of interest in fullerene polymers. Simultaneous application of high pressure and temperature on microcrystalline C_{60} powders has been subsequently shown to lead to a variety of polymerized fullerene structures.[2–7] To date, based on a simulation of powder x-ray diffraction (XRD) data, four high-pressure–high-temperature- (HPHT-) induced polymerized phases of C_{60} have been proposed: rhombohedral (R),[2–4,6] tetragonal (T),[4] orthorhombic (O),[4] and a contracted fcc (F) phase[3] (cf. Fig. 1; the F phase is not shown). Based on theoretical calculations, Nunez-Regueiro *et al.* have suggested that the application of high pressure and temperature on microcrystalline C_{60} powder can also lead to 3D polymerized structures in which the C_{60} molecules on adjacent 2D R (or T) layers may bond via hexagonal prismatic coupling.[8] Besides the photoinduced and pressure-induced polymerization of solid C_{60}, polymerization in solid C_{60} has also been reported to be induced through excitations by 1.5-keV electrons,[9] and by an ion plasma discharge.[10] Charge transfer from alkali metals (M) to C_{60} molecules in the M_1C_{60} compounds to form charged polymer chains of C_{60}^- molecules has also been proposed.[11–14]

Above the orientational ordering temperature [$T_{01} \sim 260$ K (Refs. 15–20)] solid C_{60} is a van der Waals bonded solid with a fcc crystal structure in which the individual molecules spin rapidly about random directions at each lattice site. At temperatures above T_{01} and below ~ 450 K,[21,22] oxygen-free C_{60} can be transformed by UV-visible light to a polymeric phase in which the C_{60} molecules are covalently linked to neighboring C_{60} molecules.[1] XRD studies on a series of C_{60} films exposed to successively higher doses of visible UV light showed a contraction of the fcc lattice constant from 14.17 Å (pristine) to 13.80 Å.[23] Further experiments are in progress to complete this study. The photopolymer XRD data to date suggest random intermolecular bonding within an average fcc structure. A ''2+2'' cycloaddition reaction mechanism was proposed for the covalent bonding in the C_{60} photopolymer[1,21] and subsequent HPHT polymers.[4] In this reaction, parallel double bonds on neighboring molecules are broken and reform as a four-membered ring joining the two molecules.[24] The existence of interfullerene bonds that lead to a reduced molecular symmetry in the photopolymerized phase was demonstrated using laser desorption mass spectroscopy (LDMS), infrared transmission, and Raman

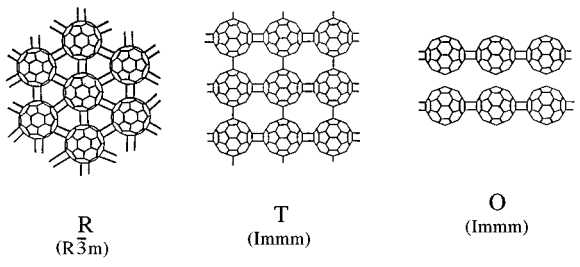

FIG. 1. Schematic structural arrangement of C_{60} molecules in the two-dimensional rhombohedral (R) and tetragonal (T) networks; and the one-dimensional orthorhombic (O) chains. The corresponding space group is also indicated below the labels for each phase. After Ref. 4.

spectroscopies.[1] Furthermore, calculations have shown that the creation of a C_{60} dimer via ''2+2'' cycloaddition is energetically favored over two isolated molecules.[25–32] Theoretical estimates of 2.4 eV (Ref. 26) and 1.6 eV (Ref. 28) were obtained for the activation energy required to break a dimer into noninteracting C_{60} monomers, in reasonable agreement with the experimental value of 1.25 eV for the photopolymer.[22] Several in-depth reviews on the experimental and theoretical studies concerning polymerization in solid C_{60} can be found in the literature.[33–37]

In the HPHT C_{60} polymers, the covalent linking between the C_{60} molecules was also proposed to be via the ''2+2'' mechanism, i.e., a four-membered ring joining adjacent molecules. From recent ''magic angle'' nuclear magnetic resonance (NMR) data[38] on the *R* and *O* polymers, the proposed four-membered ring linking C_{60} molecules was experimentally verified. Confirming evidence of covalent bonds between the C_{60} molecules in the HPHT polymers was also obtained from the LDMS spectrum[39] of a mixed phase (50% *O*+45% *T*+5% *R*) sample that was synthesized at 2 GPa and $T=350$ °C.[5] In this LDMS data,[39] a succession of ~12 clear peaks at mass numbers corresponding to $(C_{60})_N$, where $N=1,2,\ldots,12$, was observed similar to the LDMS data on the C_{60} photopolymer.[1] Furthermore, similar to the C_{60} photopolymer[1] the HPHT polymers were found insoluble in toluene. After annealing in an inert atmosphere at temperatures ~200 °C and ambient pressure, the HPHT polymers were found to depolymerize, and the C_{60} monomers again recrystallize into an fcc solid.[3,4]

Because of the weak van der Waals forces between the C_{60} molecules in the fcc pristine phase, solid C_{60} exhibits Raman and infrared intramolecular mode frequencies in good agreement with those predicted for an isolated C_{60} molecule.[40] The first infrared and Raman study of the *R* and *F* polymers was reported by Iwasa *et al.*[3] Similar to that reported earlier for the C_{60} photopolymer,[1] they observed vibrational mode splittings and concomitant mode softening of the intramolecular modes and attributed this to the formation of new intermolecular bonds. More recently, Sundar *et al.*[41] using XRD, infrared, and Raman spectroscopies have reported that C_{60} powder maintained simultaneously at 7.5 GPa and 800 °C for 6 h, readily produced the *O* phase. However, when C_{70} powder was subjected to similar experimental conditions in their apparatus, no evidence for polymerization was observed.[41] This observation is consistent with the very slow phototransformation reported for C_{70} films[42] and attributed to the reduced number (ten) of chemically reactive C═C bonds in C_{70}, which are located only in the polar caps of a C_{70} molecule, as compared to 30 uniformly distributed C═C bonds in a C_{60} molecule.

In this paper, we present a comparative infrared and Raman study of the C_{60} photopolymer and the HPHT *R*, *T*, and *O* polymers. Of the large number of modes observed in the vibrational spectra of these polymers, most of them are identified as split modes of the threefold F_{1u} infrared-active and the fivefold H_g Raman-active modes in appropriate frequency ranges. The experimental vibrational spectra are compared to corresponding calculated spectra reported for the C_{60} polymers.[26,28,30] The softening of the $A_g(2)$- and $F_{1u}(4)$-derived modes for the C_{60} photopolymer, *R*, *T*, and *O* polymers is linearly correlated with the intermolecular distance.

II. EXPERIMENTAL DETAILS

A. Synthesis of HPHT C_{60} polymers

The HPHT polymer phases were synthesized in a heated ''belt'' apparatus.[4] The *O* polymer was synthesized by heating microcrystalline C_{60} powder at ~4.8 GPa to ~250 °C for 1 h. At the same pressure, after heating to 700 °C for 2 h, the *R* polymer was obtained. Structure and phase purity in the samples were confirmed by simulations of the XRD data.[4] The pure *T* polymer phase was difficult to obtain in the pressure and temperature range of the belt apparatus. However, a mixed phase sample containing ~50% *O* and ~50% *T* polymers was prepared by maintaining C_{60} powder at 1.1 GPa and 600 °C for ~1 h. Also, from the simulations of the XRD data of these HPHT polymers, the intermolecular distance (distance between the centers of the neighboring C_{60} molecules) for the *R*, *T*, and *O* polymers were obtained as 9.20, 9.09, and 9.26 Å, respectively.[4] Finally, when C_{60} powder was simultaneously compressed (at 8.5 GPa) and heated (700 °C) for 1 h, a mixed phase sample [*R*+three dimensional (3D) prismatically coupled polymer phase] was obtained and a XRD simulation indicated that the sample was predominantly the 2D *R* polymer (80%) and only ~20% of the sample exhibited interplanar contraction required for the 3D phase (the *c* parameter for the 3D polymer is shorter than that of the 2D *R* polymer, signifying the beginning of interplanar polymerization). In this paper, the mixed phase (~50% *O* and ~50% *T*) and (~80% *R*+~20% 3D) samples will hereafter be referred as $(0.5)O+(0.5)T$ and $(0.8)R+(0.2)3D$, respectively.

Photopolymerized C_{60} samples were obtained by irradiating oxygen-free C_{60} films ($d\sim0.5$ μm) at room temperature in an inert atmosphere using a 300-W Hg arc lamp or the 514.5-nm line of an argon ion laser. Both sources induce the same changes in the vibrational spectrum. Phototransformation was monitored using the Raman-active $A_g(2)$ mode, which broadens and softens from 1469 to ~1460 cm^{-1} as the phototransformation proceeds.[1,43]

B. Spectroscopic measurements

The infrared and Raman spectra for all C_{60} polymeric samples described in this study were obtained with the samples in an inert oxygen-free atmosphere. Pressed pellets of the HPHT polymers were prepared by adding 20 wt. % KBr (for Raman measurements) and 99 wt. % KBr (for infrared transmission experiments) to the powder samples. A modified Digilab FTS-80 Fourier transform infrared (FTIR) spectrometer was used to collect the infrared transmission spectra. The Raman spectra were obtained using a 0.46-m grating spectrometer (Spex HR 460) equipped with a liquid nitrogen cooled charge-coupled device detector. A thin-film ''supernotch'' filter (Kaiser Optical, Inc.) was used to reject the stray laser light. In the Raman scattering experiments, a reduced laser flux (~20 mW/mm^2) of the 514.5-nm Ar ion laser line was employed to avoid any possible photoinduced polymerization of the samples during the measurements.

III. RESULTS AND DISCUSSION

The room-temperature infrared transmission and Raman spectra for the pristine solid C_{60}, the photopolymer, and

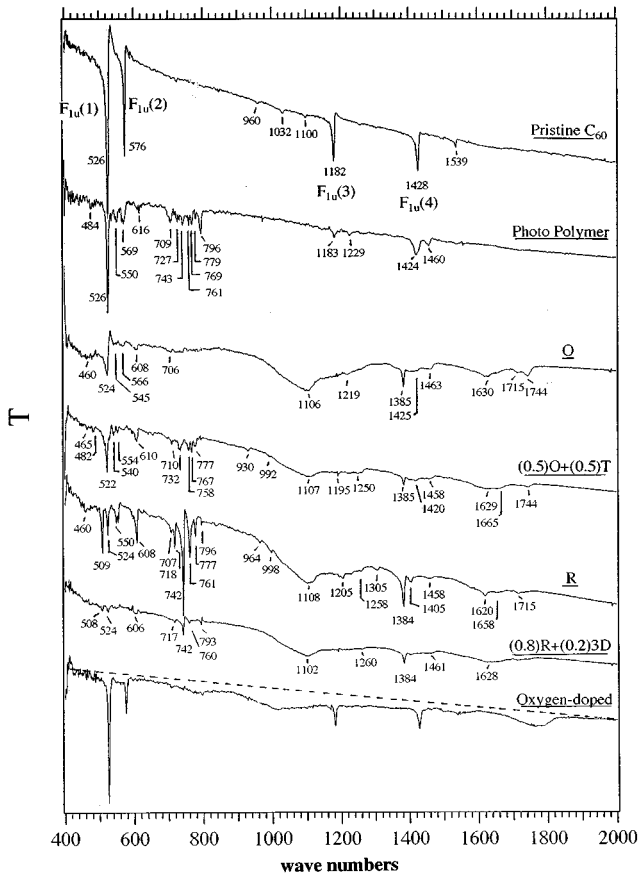

FIG. 2. Room-temperature infrared transmission spectra of pristine C_{60} compared to those of photopolymerized C_{60}, O, mixed phase $[(0.5)O+(0.5)T]$ phase, R and mixed phase $[(0.8)R+(0.2)3D]$ polymers. The infrared transmission spectrum of a C_{60} film ($d\sim5800$ Å) that was simultaneously exposed to light (488 nm, 15 mW/mm^2) and 1 atm oxygen for 25 h is also shown at the bottom of the figure. See text.

HPHT polymer samples are shown, respectively, in Figs. 2 and 3. The infrared and Raman spectra for solid C_{60} have been investigated by several groups and are well understood.[44] Consistent with the weak van der Waals intermolecular interaction, the solid state vibrational spectrum closely resembles that of C_{60} in solution[44] and in the gas phase.[45] In the spectral region below ~800 cm^{-1}, the vibrational modes are expected to be associated with predominantly radial character modes, whereas above ~800 cm^{-1}, the C_{60} vibrational modes take on a tangential character. For the pristine solid, the first-order infrared and Raman spectra in Figs. 2 and 3 exhibit, respectively, the four strong sharp infrared-active $(4F_{1u})$ lines and the ten Raman-active $(8H_g+2A_g)$ intramolecular lines predicted for the molecular I_h symmetry. The remaining relatively weaker features in the figures for pristine C_{60} are identified with overtone (2ω) or combination $(\omega_1+\omega_2)$ modes, as reported earlier.[46–48] The polarized A_g modes are nondegenerate, and the F_{1u} and H_g modes are threefold and fivefold degenerate, respectively. Under the near resonance conditions used in our Raman experiment, the strongest Raman line is the $A_g(2)$ line at 1469 cm^{-1}. This line is identified with the ''pentagonal pinch'' mode, which involves the symmetric, simultaneous contraction of the 12 pentagonal rings of the molecule. The position of this line has been shown to be sensitive to alkali-metal doping and polymerization in the solid state.[1,33,36,44,49,50] The ''breathing'' or radial $A_g(1)$ line is located at ~496 cm^{-1} (Fig. 3).

Direct evidence for covalent bonds in the HPHT polymers comes from their infrared (Fig. 2) and Raman spectra (Fig. 3). The infrared and Raman spectra for the C_{60} photopolymer have been discussed previously.[1] However, vibrational spectra on the C_{60} photopolymer with better signal-to-noise ratio are shown in Figs. 2 and 3 for comparison with that of the HPHT polymers. For the C_{60} photopolymer and the HPHT polymers, the new intermolecular bonds, as well as the concomitant changes in the *intramolecular* C-C bonding, provide a strong mechanism to break the I_h symmetry of the C_{60} molecules. This reduced symmetry activates many new infrared and Raman modes, thereby borrowing oscillator strength from the $4F_{1u}$ and $(8H_g+2A_g)$ intramolecular modes, respectively. In fact, as we discuss below, several new modes are observed, which are also clearly shifted as a result of the polymerization (Figs. 2 and 3). As the interfullerene bonds form at the expense of double bonds on the C_{60} cage, the cage is expected to soften and an overall downshift in many of the formerly ''intraball'' mode frequencies is expected. Consistent with this picture, is the experimental evidence for elongation of the *intramolecular* C-C bonds obtained from Rietveld refinements of polymeric M_1C_{60},[13] and the R, T, and O polymer phases.[4] Furthermore, consistent with XRD simulations[4] and NMR experiments,[38] the sharpness of many of the new infrared and Raman-active lines of the C_{60} polymers indicate that the C_{60} cage remains intact.

We first discuss in more detail the infrared spectra of the family of C_{60} polymers shown in Fig. 2. From top to bottom in the figure are infrared transmission spectra for C_{60}, C_{60} photopolymer, O, mixed phase $[(0.5)O+(0.5)T]$, R, and mixed phase $[(0.8)R+(0.2)3D]$ polymers. The numbers in parentheses are estimates of the fraction of the respective phase in the sample as determined from a XRD simulation. The approximate center frequency of selected absorption bands are labeled in the figure. The infrared transmission spectrum of a C_{60} film ($d\sim5800$ Å) that was simultaneously exposed to light (488 nm, 15 mW/mm^2) and 1 atm oxygen for 25 h is also shown at the bottom of the figure and will used later in the discussion of the inhomogeneously broadened features observed in Fig. 2.

The four intramolecular F_{1u}-derived modes exhibit softening and are split by the formation of interfullerene bonds. In addition to the split and downshifted F_{1u}-derived modes, several infrared-active modes are also observed in the infrared spectra of the polymers. Some give rise to relatively sharp lines and others to very broad features, for example, the continuum in the range $900<\omega<1700$ cm^{-1} in Fig. 2. It is interesting to note that the appearance of this continuum is basically the same for all pressure-induced polymers and also similar to that seen for the oxygen-doped C_{60} film (Fig. 2, bottom spectrum). We discuss this further below.

The $F_{1u}(1)$ mode in fcc pristine C_{60} is observed to broaden and soften from 526 to 522 cm^{-1} in the spectrum of the mixed $[(0.5)O+(0.5)T]$ phase polymer. This line is observed to further soften and split into two sharp lines at 509 and 524 cm^{-1} in the spectrum for the R polymer. Due to the proximity of the $F_{1u}(1)$ and $F_{1u}(2)$ modes in pristine C_{60}, it

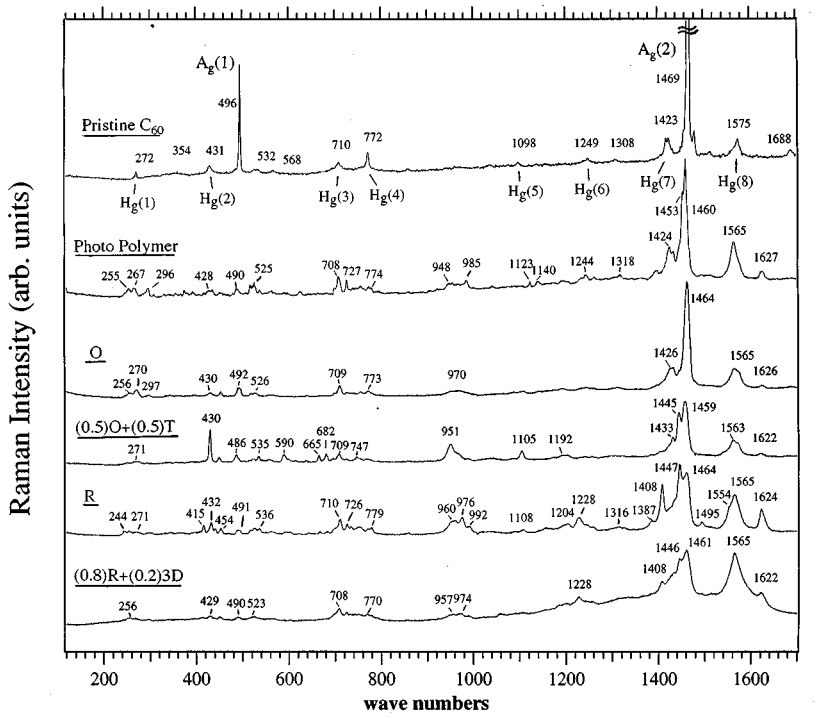

FIG. 3. Room-temperature Raman spectra for pristine C_{60} film, photopolymerized C_{60} film, and the pressure-induced polymers (see text).

is difficult to unambiguously assign the set of modes observed in the range $500<\omega<580$ cm^{-1} as split modes derived from either the $F_{1u}(1)$ or $F_{1u}(2)$ mode. The 1183- and 1229-cm^{-1} modes in the spectrum of the photopolymer are identified as split $F_{1u}(3)$-derived modes. Clear observation of the $F_{1u}(3)$-derived modes in the HPHT infrared spectra is masked by the presence of the inhomogeneously broadened feature centered $\sim$1107 cm^{-1}. We take this view for reasons discussed below, rather than to assign the very broad feature to broadened $F_{1u}(3)$-derived modes. Nevertheless, the weak mode at 1219 cm^{-1} in the *O* phase spectrum and 1205-cm^{-1} mode in the *R*-phase spectrum are identified with the softened 1229-cm^{-1} mode observed in the spectrum of the photopolymer. The infrared lines at 1424 and 1460 cm^{-1} in the spectrum of the photopolymer are identified with $F_{1u}(4)$-derived modes. In the HPHT polymers, the features between 1360 and $\sim$1480 cm^{-1} are identified as broadened $F_{1u}(4)$-derived modes. It is interesting to note that the frequency of these infrared bands matches rather well with those of the Raman bands for the same material (see Fig. 3). From group theory, it is known that the Raman and infrared active modes are no longer strictly complementary once the inversion symmetry is broken; i.e., Raman-active modes are also observed in the corresponding infrared spectrum and vice versa. In fact, weak Raman active peaks are observed in Fig. 3 at frequency positions corresponding to strong infrared-active modes. Similar arguments have been made in Rb-doped C_{60} (Rb_1C_{60}) by Martin *et al.* who proposed that the high-temperature Rb_1C_{60} phase quenched to room temperature was composed of C_{60} dimers without a center of inversion.[51]

We next discuss the new infrared-active bands in Fig. 2 that cannot be viewed approximately as F_{1u}-derived modes activated due to polymerization. The weak band at 484 cm^{-1} in the spectrum of photopolymerized C_{60} appears to broaden and soften in the HPHT polymers, except in the case of the $(0.5)O+(0.5)T$ sample where an additional, resolved weak peak centered around 482 cm^{-1} is also observed. Likewise, the 616-cm^{-1} mode is observed to soften to 608 cm^{-1} in the HPHT polymers. As can be seen in Fig. 2, the infrared intensities of the set of new modes in the range $700<\omega<800$ cm^{-1} are found quite sensitive to the particular fullerene polymer phase, exhibiting weak intensity for the 1D *O* polymer and relatively stronger intensity for the 2D *R* polymer.

The origin of the broad infrared continuum seen in the *R*, *T*, and *O* spectra may simply be caused by incomplete or disordered interfullerene bonding. The *presence* of inhomogeneously broadened lines in the infrared spectrum and their *absence* in the corresponding Raman spectrum were reported earlier[52] for a C_{60} film ($d\sim$5800 Å) that was simultaneously exposed to light (488 nm, 15 mW/mm^2) and 1 atm oxygen for 25 h. The infrared spectrum for this 25-h oxygen-doped C_{60} film is depicted at the bottom of Fig. 2. For a short exposure time, very little change in the infrared and Raman spectra over that for pristine C_{60} was observed.[52] During this period, O_2 simply diffuses into interstitial positions of the lattice, albeit the diffusion rate is accelerated dramatically by the presence of the light.[52,53] With continued exposure to light and oxygen, a chemical attack of the C_{60} cages was observed (C═O stretch at 1750 cm^{-1}) and broad infrared bands were observed[52] that are similar to the broad continuum seen in the *R*, *T*, and *O* infrared spectra. The broad infrared bands in the oxygen-doped C_{60} film were attributed to inhomogeneously broadened modes due to the variety of possible $C_{60}O_x$ molecules.[52] The overall similarity of the continuum in the infrared spectra of pressure-induced polymers and oxygen-doped C_{60} is evident in Fig. 2, although differences in the continuum are observed. Thus the broad infrared features in the HPHT polymers might stem from imperfect (i.e., random) intermolecular bonding. We might also add that the changes in the vibrational spectrum associated with photoassisted oxygen doping in C_{60} films are quite different in that (i) the $4F_{1u}$ modes do *not* exhibit mode splitting or softening and (ii) the Raman spectrum does *not*

exhibit the broad continuum, such as the one observed for the $(0.8)R+(0.2)$3D sample in Fig. 3.

Returning to Fig. 3, we make further comments about the Raman spectra of the C_{60} polymers. Approximate center frequencies for selected Raman peaks are indicated in the figure. The strongest Raman line at 1469 cm^{-1} in pristine C_{60} (pentagonal pinch mode) is observed downshifted to 1460 cm^{-1} in the spectrum for photopolymerized C_{60}. As noted in previous work, this band loses intensity and becomes depolarized.[43,50] It is clear that the Raman spectra of the HPHT polymers are similar to that observed for the photopolymer. However, differences exist that need to be elucidated theoretically. As was the case for the F_{1u} modes, pressure-induced polymerization appears to induce a splitting of the fivefold degenerate H_g modes. In addition, new Raman lines that cannot be viewed as H_g-derived modes are also observed in Fig. 3. Furthermore, the Raman spectrum for the $(0.8)R+(0.2)$3D sample is quite similar to that observed for the R polymer, although the Raman peaks in the former are broadened and accompanied with a broad continuum in the frequency region in the range $800<\omega<1700$ cm^{-1}. Thus it is difficult to assign any Raman feature in this sample with the 3D component. The origin of this broad continuum in the Raman spectrum for the $(0.8)R+(0.2)$3D sample might signal the presence of some broken C_{60} cages produced under the extreme synthesis conditions. Broken C_{60} cages would also give rise to a broad background in the XRD data.

The set of lines in the range $200<\omega<300$ cm^{-1} in Fig. 3 can be thought of as $H_g(1)$-derived modes. Likewise, the set of Raman-active lines in the range $400<\omega<460$ cm^{-1} are assigned to modes that result from the splitting of the $H_g(2)$ mode at 431 cm^{-1} in pristine C_{60}. While the $H_g(1)$-derived modes in the photopolymer and O spectra, and the $H_g(2)$-derived modes in the R spectrum are well resolved, other $H_g(1)$- and $H_g(2)$-derived modes are somewhat broadened. The $H_g(2)$-derived peak at 430 cm^{-1} is particularly intense in the Raman spectrum of the $(0.5)O+(0.5)T$ phase. The nondegenerate $A_g(1)$ mode is found to soften from 496 cm^{-1} in pristine C_{60} to $\sim$490 cm^{-1} in the spectrum of the R polymer. Raman lines in the frequency regions $700<\omega<800$ cm^{-1} and $1100<\omega<1280$ cm^{-1} are assigned, respectively, to the $H_g(3)$- and $H_g(4)$-derived and the $H_g(5)$- and $H_g(6)$-derived modes. Similarly, the Raman-active modes in the frequency region $1350<\omega<1600$ cm^{-1} can be identified as $H_g(7)$- and $H_g(8)$-derived modes and the strongest peak in this region corresponds to the $A_g(2)$-derived mode. Finally in Fig. 3, the observation of Raman-active modes that are *not* H_g-derived modes is particularly evident in the frequency range $900<\omega<1000$ cm^{-1}, and the intensity of these modes is sensitive to the particular structure of the fullerene polymer.

Theoretical calculations of the frequencies and intensities of the infrared- and Raman-active vibrational modes in C_{60} dimers, trimers, and infinite one-dimensional polymeric chains have been reported in the literature. While several groups have calculated the vibrational mode frequencies,[25,26,28,29] only Adams *et al.*[26,30] and Porezag *et al.*[28] have also obtained the intensity of the Raman-active modes. To our knowledge, the calculated infrared intensities have been reported only for the C_{60} dimer.[30] In Fig. 4, the theoretical infrared absorption spectra of C_{60} and the C_{60} dimer (shown as inset figures) calculated Adams *et al.*[30] are compared to the experimental absorption spectrum for the pristine and photopolymerized C_{60}. A smooth sloping background was removed from the experimental transmission (T) data and the results are plotted as an optical density $[\log_{10}(1/T)]$ versus frequency. The theoretical absorption peaks in the inset figures have been artificially broadened into Lorentzians with 1 cm^{-1} for the full width at half maximum (FWHM) peak intensity.

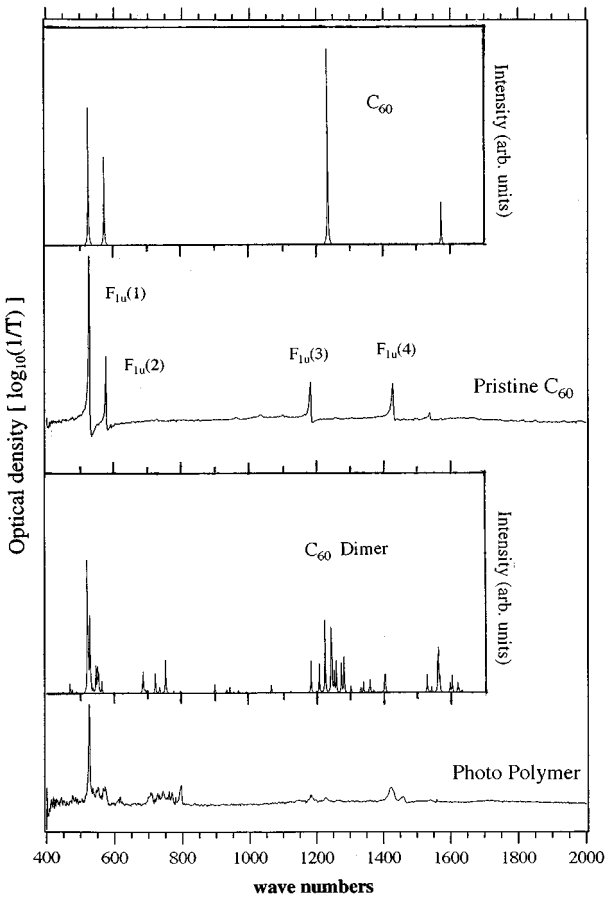

FIG. 4. Comparison of the experimental infrared optical density of pristine C_{60} and photopolymerized C_{60} to the calculated spectra of C_{60} and C_{60} dimers [insets (see Ref. 30)]. The calculated infrared absorption peaks have bean artificially broadened into Lorentzians of 1 cm^{-1} for the FWHM peak intensity.

Comparing first the calculated and experimental results for C_{60}, we see that the four F_{1u} modes are reproduced in reasonably good agreement with experiment, except for the relative intensity of the $F_{1u}(3)$ mode. The calculated $F_{1u}(3)$ and $F_{1u}(4)$ mode frequencies are also noticeably higher than the corresponding experimental frequencies by $\sim$40 and $\sim$120 cm^{-1}, respectively.[30] It is therefore reasonable to expect that the calculated dimer spectrum exhibits similar disagreement compared to the experiment. Thus for the $F_{1u}(3)$-derived modes, the calculated intensities would be expected to be too intense and the calculated frequencies to be somewhat higher. While it is tempting to say that the calculated dimer frequencies and intensities are in qualitative agreement with the photopolymer spectrum, it must be appreciated that many of the experimental photopolymer lines

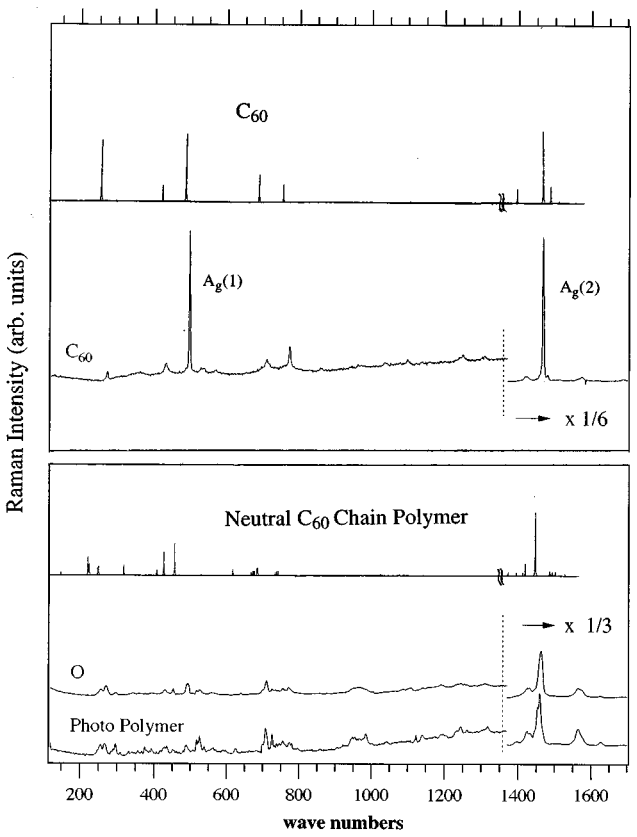

FIG. 5. Upper panel: Comparison of the experimental Raman spectrum of pristine C_{60} to the calculated Raman spectrum reported by Adams *et al.* (Ref. 26) (see text). Lower panel: Comparison of the experimental Raman spectrum of the *O* polymer and the photopolymer to the calculated Raman spectrum for an infinitely long 1D C_{60} polymer chain (Refs. 26 and 30) (see text). In both panels, the calculated Raman peaks have been artificially broadened into Lorentzians of 1 cm^{-1} for the FWHM peak intensity.

are much broader than observed in solid C_{60}. It is therefore possible that these broad features simply stem from inhomogeneous broadening due to the formation of a range of higher oligomers, consistent with the LDMS data[1,54] and XRD data.[23] It should be emphasized that the structure of the photopolymer is still under study. Based on a comparison of the calculated electronic and vibrational states for the C_{60} dimer by Adams *et al.*[26] to their experimental ultraviolet photoemission spectroscopy (UPS) and vibrational data of laser modified thin ($d \sim 400$ Å) C_{60} films, Lopinski, Fox, and Lannin[55] have suggested that the photopolymerized C_{60} is predominantly comprised of dimers, and trimers to a small extent. However, a distribution of $(C_{60})_N$ clusters for $N=1, \ldots, 20$, has been observed in the LDMS studies of the photopolymer[1,54] and interpreted as evidence for covalent bonding between molecules in these large clusters. In our opinion, this LDMS observation remains inconsistent with the ''dimer'' model for the photopolymer.

In Fig. 5, the calculated and experimental Raman spectrum for solid C_{60} appears in the upper panel. In the lower panel of the figure, the calculated Raman spectrum for a neutral chain polymer comprised of C_{60} cages connected by four membered rings is compared with the spectra for the photopolymer and the *O* polymer. The calculated Raman intensities in the inset figures were obtained using the first-principles force constants together with the bond-charge polarizability parameters appropriate for describing nonresonance Raman scattering intensities.[30,56] For the benchmark C_{60} solid, the calculated and experimental frequencies compare well except for the high-frequency tangential modes. The calculated C_{60} frequencies are found ~ 130 cm^{-1} higher than the corresponding experimental frequencies for the high-frequency Raman-active modes. Furthermore, the calculated C_{60} intensities are not in good agreement with experiment since the calculations employed the bond polarizability parameters reported for nonresonant scattering.[30,56] The Raman data shown in Figs. 3 and 5 were collected at near-resonance. In Fig. 5, to facilitate better comparison of the calculated mode frequencies to the experimental high-frequency tangential modes, the calculated spectra above ~ 1350 cm^{-1} were intentionally downshifted in frequency by 130 cm^{-1}. Note that the experimental Raman intensities have also been suitably scaled above 1350 cm^{-1}. Since the bond charge model (nonresonance) predicts that the intensities of the $A_g(1)$ and $A_g(2)$ lines for pristine C_{60} are nearly the same (upper panel), we can probably assume that the theory will underestimate the intensity of the $A_g(2)$-derived mode in the Raman spectra for polymers (bottom panel). Taking this view we compare the calculated results for the neutral polymer chain to that obtained experimentally for the HPHT *O* polymer and the photopolymer. Qualitatively, theory is seen to be in good agreement with experiment; i.e., regions of theoretical and experimental Raman activity are in qualitative agreement. Although one might expect the *O* polymer to be reasonably well described by the theoretical model, the photopolymer is not thought to exhibit polymeric chain structures.[23] At this point, it may be best to simply state that the calculated Raman spectrum of a neutral C_{60} chain polymer is in qualitative agreement with both the *O* and photopolymer experimental data. Insofaras the photopolymer is concerned, further structural studies are needed to prove or disprove the presence of oligomer chains. It should be noted that the infrared spectra of these two polymer phases are very different. Therefore, it is much too early to give serious consideration to oligomer chain formation in the photopolymer.

Since the Raman spectra in the vicinity of the pentagonal pinch mode are distinct for each of the polymeric phases, the spectra are reproduced in Fig. 6 on an expanded frequency scale. The data in the figure are represented by dots and the solid curves through the data represent the results of Lorentz oscillator fits to the data. Since the phase purity in the sample was inferred from the XRD measurements, the Raman spectrum for the *T* polymer in Fig. 6 was calculated simply by subtraction of the Raman spectrum for the *O* polymer from that measured for the $(0.5)T+(0.5)O$ sample. Individual Lorentz oscillators are shown below the data superimposed on a flat background and the Lorentzians are intentionally displaced downward for clarity. The center frequencies for the Lorentz oscillators in the spectra of HPHT polymers are observed very nearly at the same frequency; only the relative intensities change. The frequencies are ~ 1408, ~ 1424, ~ 1433, ~ 1446, ~ 1458, and ~ 1464 cm^{-1} and the width (FWHM) of these oscillator are listed in Table I. In Fig. 6, the strongest Raman line for the *R* (and also *T*) polymer is observed around 1445 cm^{-1}, in good agreement with 1447

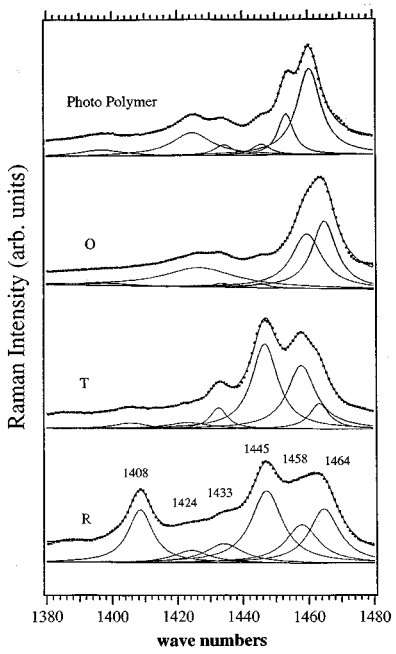

FIG. 6. Raman spectra for the photopolymer and the HPHT polymers in the vicinity of the pentagonal pinch mode frequency. The dots represent the experimental data and the solid curve through the data is a result of a Lorentzian line-shape analysis. Individual Lorentz oscillators (see Table I) for each spectrum are shown below the data superimposed on a flat background.

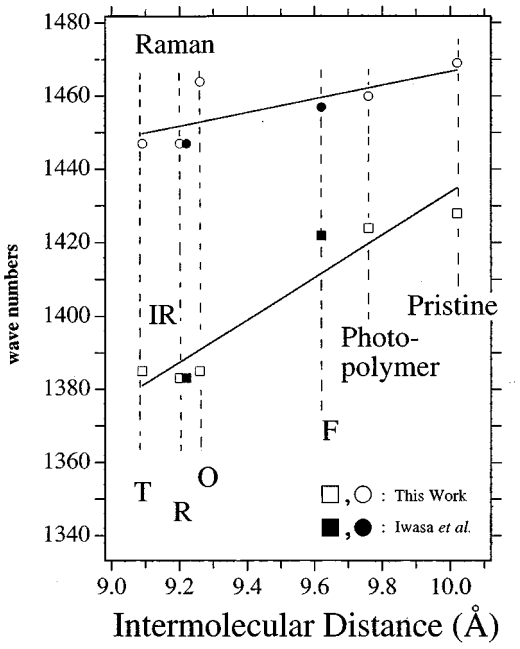

FIG. 7. Plot of frequency positions for the $A_g(2)$- and $F_{1u}(4)$-derived modes in the polymeric phases vs the corresponding intermolecular distances. The solid inclined lines represent the linear least-squares fits to the data described here and those reported by Iwasa *et al.* (Ref. 3).

cm^{-1} reported for the *R* polymer in Ref. 3. However, the frequency position of the strongest Raman line for the *O* polymer (1464 cm^{-1}) is found ~4 cm^{-1} upshifted from the frequency position (1460 cm^{-1}) reported for the *O* polymer by Sundar *et al.*[41] It should be remarked that the synthesis conditions for the *O* polymer adopted in Ref. 41 (7.5 GPa and 800 °C for 6 h) are drastically different from those used in this study (~4.8 GPa and ~250 °C for 1 h). Furthermore, since they did not report a detailed line-shape analysis, their reported frequencies may differ slightly from ours reported here. The weak Raman peak at 1445 cm^{-1} in the *O* phase spectrum (cf. Fig. 6) was observed as a relatively strong shoulder to the 1460-cm^{-1} peak in the Raman spectra reported in Ref. 41.

If it is assumed that the strongest peak in the Raman spectra for the polymeric phases is always basically the same $A_g(2)$-derived mode, then a plot of mode frequency as a function of the intermolecular separation (a_I) has physical meaning. This plot is displayed in Fig. 7 along with a similar plot for the strongest $F_{1u}(4)$-derived mode. The shift to lower frequency for the pentagonal pinch mode has been modeled using molecular dynamics for a C_{60} dimer, trimer, and higher oligomers.[26,28] A downshift of ~10 cm^{-1} for the $A_g(2)$-derived mode frequency was predicted for the C_{60} dimer and trimer; and another peak downshifted by ~20 cm^{-1} was predicted for longer C_{60} polymers.[28] The upper line shown in Fig. 7 is a least-squares fit to the data for the $A_g(2)$-derived mode frequency versus a_I and the lower line is the fit to the $F_{1u}(4)$-derived mode. The values for the frequency position and the intermolecular distance for the *F* phase were obtained from Ref. 3. The least-squares fit yields $\Delta\omega/\Delta a_I \sim 19$ cm^{-1}/Å for the $A_g(2)$-derived mode, a value of $\Delta\omega/\Delta a_I \sim 58$ cm^{-1}/Å is obtained for the $F_{1u}(4)$-derived mode. For comparison, the $A_g(2)$-derived mode and the $F_{1u}(4)$-derived mode frequencies in the alkali metal (*M*) doped C_{60} (M_xC_{60}) exhibit, respectively, a softening of 6 and 14 cm^{-1} per electron transferred from the alkali metal to the C_{60} molecule.[50]

TABLE I. Experimentally determined Raman-active frequencies in cm^{-1} for photopolymerized C_{60} and HPHT polymers. The numbers within the parentheses correspond to the full width at half maximum (FWHM) intensity linewidths in cm^{-1}.

Photopolymer	*R*	*O*	*T*
1396 (8)		1399(10)	
	1408 (4)		1407(10)
1424 (7)	1424 (6)	1426(13)	1424 (8)
1434 (3)	1434 (7)	1433 (3)	1433 (3)
1446 (3)	1447 (6)	1445 (3)	1446 (5)
1453 (3)			
1460 (4)	1458 (6)	1460 (5)	1458 (5)
	1464 (5)	1464 (4)	1464 (5)

IV. CONCLUSIONS

The interfullerene bonds provide a strong mechanism to break the icosahedral symmetry of an isolated C_{60} molecule, thus revealing rich infrared and Raman spectra for the fullerene polymers. As a result, all the Raman-active H_g modes and infrared-active F_{1u} modes are visibly split in the experiment and theoretical spectra. Furthermore, most of these modes are softened relative to their counterparts in pristine C_{60} and this is attributed to the loss of double bonds

in the C_{60} cages, which have been broken to form four-membered intermolecular rings. The calculated vibrational spectra for C_{60}, C_{60} dimer, and the C_{60} infinite polymer chain were found in qualitative agreement with the experimental spectra for pristine C_{60}, photopolymer, and the *O* polymer, respectively, yet the infrared data for the *O* polymer and photopolymer are quite different. The overall similarity between the Raman spectra of the *O* polymer and the photopolymer suggests that the photopolymer may be composed of polymer chains but further structural work is necessary in the photopolymer to substantiate the presence of chain oligomers. A frequency softening of $\Delta\omega/\Delta a_I \sim 58$ cm^{-1}/Å and ~ 19 cm^{-1}/Å is estimated, respectively, for the $F_{1u}(4)$- and the $A_g(2)$-derived modes. Since these polymeric systems are quite complex structurally, theoretical calculations of the infrared and Raman spectra for each polymeric phase will be required to interpret quantitatively the experimental results. Further experimental work is needed to identify the low-frequency ($\omega \leqslant 200$ cm^{-1}) infrared and Raman modes of these C_{60} polymers, as these modes most directly probe the nature of the intermolecular coupling.

Note added in proof. Recently, further simulations of the XRD data of the orthorhombic polymer indicated the presence of disorder in the sample. This has been identified with variable polymer chains as well as possible ''bifurcation'' of these chains. These XRD simulations indicate that the intermolecular distance (a_I) is 9.26 Å, instead of the expected value of 9.1 Å. Furthermore, we found that a more ordered orthorhombic phase with $a_I = 9.07$ Å coexists with the tetragonal phase, as, for example, in the ($0.5\,O + 0.5\,T$) sample used in this study.

ACKNOWLEDGMENTS

The work at the University of Kentucky was supported by NSF OSR-9452895 and the Center for Applied Energy Research. The authors wish to thank Dr. Gary B. Adams and Professor J. B. Page for communicating their calculated infrared spectra for C_{60} and C_{60} dimers prior to publication.

[1] A. M. Rao *et al.*, Science **259**, 955 (1993).
[2] O. Bethoux *et al.*, in *Proceedings of the Materials Research Society, Boston, 1993, Abstracts of Contributed Papers* (Materials Research Society, Pittsburgh, 1993). Abstract No. G2.9, p. 202.
[3] Y. Iwasa *et al.*, Science **264**, 1570 (1994).
[4] M. Nunez-Regueiro *et al.*, Phys. Rev. Lett. **74**, 278 (1995).
[5] I. O. Bashkin *et al.*, J. Phys. Condens. Matter **6**, 7491 (1994).
[6] G. Oszlanyi and L. Forro, Solid State Commun. **93**, 265 (1995).
[7] Q. Zhu, Phys. Rev. B **52**, R723 (1995).
[8] M. Nunez-Regueiro *et al.* (unpublished).
[9] Y. B. Zhao *et al.*, Appl. Phys. Lett. **64**, 577 (1994).
[10] N. Takahashi *et al.*, J. Appl. Phys. **74**, 5790 (1993).
[11] J. Winter and H. Kuzmany, Solid State Commun. **83**, 1321 (1992).
[12] S. Pekker *et al.*, Science **265**, 1077 (1994).
[13] P. W. Stephens *et al.*, Nature **370**, 636 (1994).
[14] O. Chauvet *et al.*, Phys. Rev. Lett. **72**, 2721 (1994).
[15] P. A. Heiney *et al.*, Phys. Rev. Lett. **66**, 2911 (1991).
[16] P. A. Heiney, J. Phys. Chem. Solids **53**, 1333 (1992).
[17] W. I. F. David *et al.*, Europhys. Lett. **18**, 219 (1992).
[18] R. Tycko *et al.*, Phys. Rev. Lett. **67**, 1886 (1991).
[19] R. D. Johnson, D. S. Bethune, and C. S. Yannoni, Acc. Chem. Res. **25**, 169 (1992).
[20] W. I. F. David *et al.*, Nature **353**, 147 (1991).
[21] P. Zhou *et al.*, Chem. Phys. Lett. **211**, 337 (1993).
[22] Y. Wang *et al.*, Chem. Phys. Lett. **217**, 413 (1994).
[23] P. W. Stephens (private communication).
[24] K. Venkatesan and V. Ramamurthy, *Bimolecular Photoreactions in Crystals. Photochemistry in Organized and Constrained Media* (VCH, New York, 1991), Chap. 4, p. 133.
[25] M. Menon, K. R. Subbaswamy, and M. Sawtarie, Phys. Rev. B **49**, 13 966 (1994).
[26] G. B. Adams *et al.*, Phys. Rev. B **50**, 17 471 (1994).
[27] M. R. Pederson and A. A. Quong, Phys. Rev. Lett. **74**, 2319 (1995).
[28] D. Porezag *et al.*, Phys. Rev. B **52**, 14 963 (1995).
[29] D. L. Strout *et al.*, Chem. Phys. Lett. **214**, 576 (1993).
[30] G. B. Adams and J. B. Page, in Fullerene Polymers and Fullerene-Polymer Composites, edited by P. C. Eklund and A. M. Rao (Springer-Verlag, Berlin, in press), Chap. 5
[31] N. Matsuzawa *et al.*, J. Phys. Chem. **98**, 2555 (1994).
[32] J. Fagerstrom and S. Stafstrom, Phys. Rev. B **53**, 13 150 (1996).
[33] P. C. Eklund *et al.*, Thin Solid Films **257**, 185 (1995).
[34] Y. Iwasa, *Optical Properties of Low Dimensional Materials*, edited by T. Ogawa and Y. Kanemitsu (World Scientific, Singapore, 1995).
[35] Fullerene Polymers and Fullerene-Polymer Composites (Ref. 30).
[36] M. S. Dresselhaus, G. Dresselhaus, and P. C. Eklund, J. Raman Spect. **27**, 351 (1996).
[37] A. M. Rao and P. C. Eklund, Cluster Assembled Materials, edited by K. Sattler (Trans Tech Publications, Aedermannsdorf, in press).
[38] C. Goze *et al.*, Phys. Rev. B **54**, R3676 (1996).
[39] A. M. Rao *et al.* (unpublished).
[40] G. Dresselhaus, M. S. Dresselhaus, and P. C. Eklund, Phys. Rev. B **45**, 6923 (1992).
[41] C. S. Sundar *et al.*, Phys. Rev. B **53**, 8180 (1996).
[42] A. M. Rao *et al.*, Chem. Phys. Lett. **224**, 106 (1994).
[43] P. Zhou *et al.*, Appl. Phys. Lett. **60**, 2871 (1992).
[44] M. S. Dresselhaus, G. Dresselhaus, and P. C. Eklund, in *Science of Fullerenes and Carbon Nanotubes* (Academic, New York, 1996), Chap. 11.
[45] J. M. Holden (unpublished).
[46] K.-A. Wang *et al.*, Phys. Rev. B **48**, 11 375 (1993).
[47] Z. H. Dong *et al.*, Phys. Rev. B **48**, 2862 (1993).
[48] M. C. Martin, D. Koller, and L. Mihaly, Phys. Rev. B **50**, 6538 (1994).
[49] P. C. Eklund *et al.*, Thin Solid Films **257**, 211 (1995).
[50] P. C. Eklund *et al.*, J. Phys. Chem. Solids **53**, 1391 (1992).
[51] M. C. Martin *et al.*, Phys. Rev. B **51**, 3210 (1995).
[52] A. M. Rao *et al.*, J. Mat. Res. **8**, 2277 (1993).
[53] C. C. Eloi *et al.*, J. Mat. Res. **8**, 3085 (1994).
[54] D. S. Cornett *et al.*, J. Phys. Chem. **97**, 5036 (1993).
[55] G. P. Lopinski, J. R. Fox, and J. S. Lannin, Chem. Phys. Lett. **239**, 107 (1995).
[56] S. Guha *et al.*, Phys. Rev. B **53**, 13 106 (1996).